Weinberg's 3HDM potential with spontaneous *CP* violation

R. Plantey,[1,*] O. M. Ogreid,[2,†] P. Osland,[3,‡] M. N. Rebelo,[4,§] and M. Aa. Solberg[1,‖]

[1]*Department of Structural Engineering, NTNU, 7491 Trondheim, Norway*
[2]*Western Norway University of Applied Sciences, Postboks 7030, N-5020 Bergen, Norway*
[3]*Department of Physics and Technology, University of Bergen, Postboks 7803, N-5020 Bergen, Norway*
[4]*Centro de Física Teórica de Partículas—CFTP and Departamento de Física, Instituto Superior Técnico—IST, Universidade de Lisboa, Avenida Rovisco Pais, P-1049-001 Lisboa, Portugal*

(Received 14 April 2023; accepted 3 October 2023; published 30 October 2023)

We study the potential of Weinberg's $\mathbb{Z}_2 \times \mathbb{Z}_2$-symmetric three-Higgs-doublet model. The potential is designed to accommodate *CP* violation in the scalar sector within a gauge theory, while at the same time allowing for natural flavor conservation. This framework allows for both explicit and spontaneous *CP* violation. *CP* can be explicitly violated when the coefficients of the potential are taken to be complex. With coefficients chosen to be real, *CP* can be spontaneously violated via complex vacuum expectation values (VEVs). In the absence of the terms leading to the possibility of *CP* violation, either explicit or induced by complex VEVs, the potential has two global $U(1)$ symmetries. In this case, spontaneous symmetry breaking would, in general, give rise to massless states. In a realistic implementation, those terms must be included, thus preventing the existence of Goldstone bosons. A scan over parameters, imposing the existence of a neutral state at 125 GeV that is nearly *CP* even shows that, in the absence of fine-tuning, the scalar spectrum contains one or two states with masses below 125 GeV that have a significant *CP*-odd component. These light states would have a low production rate via the Bjorken process and could thus have escaped detection at the Large Electron-Positron Collider. At the LHC, the situation is less clear. While we do not here aim for a full phenomenological study of the light states, we point out that the $\gamma\gamma$ decay channel would be challenging to measure because of suppressed couplings to WW.

DOI: 10.1103/PhysRevD.108.075029

I. INTRODUCTION

In the Standard Model (SM) there is only one Higgs doublet and *CP* cannot be violated in the scalar sector. With the addition of one extra Higgs doublet, *CP* can be violated in this sector both explicitly, via the introduction of complex coefficients or spontaneously as was shown by Lee [1]. Spontaneous *CP* violation puts the breaking of *CP* and electroweak symmetry breaking on equal footing. However, the Yukawa couplings of models with two or more Higgs doublets lead to potentially dangerous flavor-changing neutral currents (FCNCs), for which there are stringent experimental limits. In order to solve this problem for the two-Higgs-doublet model, a solution was proposed [2,3], based on the imposition of natural flavor conservation (NFC) resulting from an additional $\mathbb{Z}_2$ symmetry in the scalar and in the Yukawa sector, forcing all the right-handed quarks of each sector only to couple to a single Higgs doublet, thus eliminating FCNCs at the tree level. However, imposing a discrete symmetry on the scalar potential in the context of two-Higgs-doublet models automatically leads to *CP* conservation. This can be evaded by adding a term softly breaking the $\mathbb{Z}_2$ symmetry, in which case *CP* can be spontaneously violated [4]. In 1976, it was pointed out by Weinberg [5] that the scalar potential of models with three Higgs doublets and with additional $\mathbb{Z}_2$ symmetries leading to NFC can violate *CP* explicitly and can also provide a mechanism for naturally small *CP* violation. Soon afterward, Branco [6] showed that this framework also allows for the possibility of spontaneous *CP* violation.

In this work we outline some important features of the Weinberg potential with real coefficients and *CP* violation, with an emphasis on the mass spectrum. A more detailed phenomenological analysis will be presented elsewhere. In particular, we will demonstrate that there are regions of

*Robin.Plantey@ntnu.no
†omo@hvl.no
‡Per.Osland@uib.no
§rebelo@tecnico.ulisboa.pt
‖Marius.Solberg@ntnu.no

parameter space where the electron electric dipole moment is below $10^{-29}\ e \cdot \mathrm{cm}$, as required by experiments [7]. This is an important constraint on *CP*-violating three-Higgs-doublet models (3HDMs).

It is also important to point out that the requirements of spontaneous *CP* breaking and NFC lead to a class of theories where *CP* nonconservation is solely due to Higgs exchange [8]. The fact that the right-handed quarks of each sector only couple to a single Higgs doublet allows for the rephasing of the right-handed quarks in such a way as to cancel the phase of the vacuum expectation value (VEV) of the doublet to which these quarks couple, thus leading to a real Cabibbo-Kobayashi-Maskawa (CKM) matrix. It is by now experimentally established that the CKM matrix is complex [9,10], implying that if one wants to build a fully realistic model from the point of view of flavor this issue must be addressed. To solve this problem one might, for instance, consider scenarios with the addition of vectorlike quarks [11,12].

We consider the explicitly *CP*-conserving $\mathbb{Z}_2 \times \mathbb{Z}_2$-symmetric[1] Weinberg potential [5], following the notation of Ivanov and Nishi [13],

$$V = V_2 + V_4, \quad \text{with} \quad V_4 = V_0 + V_{\mathrm{ph}}, \tag{1.1a}$$

where V_2 and V_0 are insensitive to independent rephasing of the Higgs doublets,

$$V_2 = -\left[m_{11}(\phi_1^\dagger\phi_1) + m_{22}(\phi_2^\dagger\phi_2) + m_{33}(\phi_3^\dagger\phi_3)\right], \tag{1.1b}$$

$$\begin{aligned} V_0 = {} & \lambda_{11}(\phi_1^\dagger\phi_1)^2 + \lambda_{12}(\phi_1^\dagger\phi_1)(\phi_2^\dagger\phi_2) + \lambda_{13}(\phi_1^\dagger\phi_1)(\phi_3^\dagger\phi_3) \\ & + \lambda_{22}(\phi_2^\dagger\phi_2)^2 + \lambda_{23}(\phi_2^\dagger\phi_2)(\phi_3^\dagger\phi_3) + \lambda_{33}(\phi_3^\dagger\phi_3)^2 \\ & + \lambda'_{12}(\phi_1^\dagger\phi_2)(\phi_2^\dagger\phi_1) + \lambda'_{13}(\phi_1^\dagger\phi_3)(\phi_3^\dagger\phi_1) \\ & + \lambda'_{23}(\phi_2^\dagger\phi_3)(\phi_3^\dagger\phi_2), \end{aligned} \tag{1.1c}$$

whereas

$$V_{\mathrm{ph}} = \lambda_1(\phi_2^\dagger\phi_3)^2 + \lambda_2(\phi_3^\dagger\phi_1)^2 + \lambda_3(\phi_1^\dagger\phi_2)^2 + \mathrm{H.c.} \tag{1.1d}$$

would be sensitive to rephasing of the doublets. Explicit *CP* conservation means that it is possible to make $\lambda_1, \lambda_2, \lambda_3$ real by a rephasing of the scalar doublets. In this case *CP* violation can only occur spontaneously, i.e., via complex VEVs. For simplicity, in our discussion we choose to work in this basis.

In the limit of $\{\lambda_1, \lambda_2, \lambda_3\} \to 0$ (or $V_{\mathrm{ph}} \to 0$), the potential acquires two[2] $U(1)$ symmetries, since both V_2 and V_0 are insensitive to rephasing of the fields. It is the emergence of an additional symmetry that would allow for these terms to be removed from the potential in a consistent way. Different symmetries of multi-Higgs models occur frequently and play an important role. As is clear from the classification in Ref. [14], the full additional symmetry in this limit is simply the $U(1) \times U(1)$ symmetry we are seeing here. Starting from the general Weinberg potential, two of the scalar masses tend to zero when we approach the limit where these $U(1)$ global symmetries emerge and are broken by the vacuum.[3]

Experimentally, an SM-like scalar (h_{SM}) has been observed at 125.25 GeV with trilinear $h_{\mathrm{SM}}VV$ ($V = W, Z$) gauge couplings that have very little *CP*-odd "contamination" [16,17]. One way to arrive at this situation is for the coefficients of the phase-sensitive terms of the potential to be small. In the limit when these terms vanish, *CP* is conserved and the physical scalars have definite *CP* parities. As stated earlier, there will also be two massless states in this limit, as long as all VEVs are nonzero.

At this point, it is useful to comment on "natural" alignment, when the $h_{\mathrm{SM}}VV$ coupling automatically attains full strength due to the symmetry of the potential. Pilaftsis has shown [18] (see also Ref. [19]) that this happens in a 3HDM if the quartic part of the potential has an Sp(6), SU(3), or $\mathrm{SO}(3) \times CP$ symmetry. Another possibility is to have an unbroken $\mathbb{Z}_2 \times \mathbb{Z}_2$ symmetry. In our framework we require *CP* to be broken spontaneously. In order to have *CP* violation λ_1, λ_2, and λ_3 must be simultaneously nonzero and all VEVs must be different from zero. The latter breaks the $\mathbb{Z}_2 \times \mathbb{Z}_2$ symmetry. Therefore, there is no natural alignment in this case. Since both the Weinberg $\mathbb{Z}_2 \times \mathbb{Z}_2$-symmetric potential and the $U(1) \times U(1)$-symmetric limit contain terms not compatible with these higher symmetries, it follows that natural alignment is not available in the present framework. In particular, we note that *CP* violation is not compatible with natural alignment.

In this work, we instead enforce alignment as a constraint on the parameters, leaving room for small deviations.

In view of the above discussion, it is interesting to explore whether the spectrum will contain two light states, lighter than the one whose trilinear hVV gauge coupling is SM-like. What we will see in our parameter scans is the following feature:

In a realistic case, i.e., with an SM-like Higgs boson at $m_h = 125.25$ GeV, the scenario where the SM-like scalar is the lightest requires fine-tuning. That is, in the bulk of the acceptable parameter space, lighter neutral scalars are

[1]The potential is separately symmetric under $\phi_i \to -\phi_i$ for all three ϕ_i, which means that there are in fact three $\mathbb{Z}_2$ symmetries.

[2]The third $U(1)$ symmetry can be absorbed in the $U(1)$ hypercharge symmetry.

[3]The masses are continuous functions of the couplings of the phase-sensitive part of the potential: The masses squared are the roots of the characteristic polynomial of the mass-squared matrix. The coefficients of this characteristic polynomial will be polynomials in the couplings of the phase-sensitive part of the potential, i.e., continuous functions of these couplings. Moreover, the roots of a polynomial are continuous functions of the coefficients (see, e.g., [15]), so then the masses squared are continuous functions of the phase-sensitive couplings.

predicted. These generally have a considerable *CP*-odd content.

Moreover, those light states would have suppressed trilinear gauge couplings $h_i WW$ and $h_i ZZ$ ($i = 1, 2$), since these couplings are constrained by the orthogonality of the mixing matrix; hence they may have escaped detection at the Large Electron-Positron Collider (LEP).

The paper is organized as follows. In Sec. II we minimize the Weinberg potential, and discuss *CP* conservation and properties of the mass matrices, introducing at the same time notation and definitions used in the remainder of the article. Section III presents the couplings among the electroweak gauge bosons and the scalars, and Sec. IV presents the Yukawa couplings. Then, in Sec. V we present results of a scan over the potential parameters, subject to a set of well-established constraints. In Sec. VI we compare two ways of accommodating the discovered SM-like Higgs particle in this potential, with either one or two states being lighter. Finally, Sec. VII contains concluding remarks. The expressions for the mass-squared matrices and pseudo-Goldstone masses are given in Appendix A and a simple version of the model, which turns out to conserve *CP*, is discussed in Appendix B.

II. GENERAL PROPERTIES OF THE WEINBERG POTENTIAL

We give here some basic properties of the minimum of the potential and comment on conditions for *CP* conservation. Such conditions can be analyzed from the point of view of *CP*-odd scalar basis invariants [20,21] (see also Ref. [22]), but a complete discussion is beyond the scope of this work and will be presented elsewhere. We will here only note that *CP* is conserved whenever any coupling in $V_{\rm ph}$ vanishes (provided all VEVs are nonzero) or $\sin(2\theta_2 - 2\theta_3) = 0$.[4]

A. Minimizing the potential

By an overall phase rotation, we choose the VEV of ϕ_1, $w_1 \equiv v_1$ real, whereas the other VEVs, w_2 and w_3 will, in general, be complex. We introduce phases θ_i by

$$w_i = v_i e^{i\theta_i}, \quad i = 2, 3, \tag{2.1}$$

with $v_1^2 + v_2^2 + v_3^2 = v^2$ and $v = 246$ GeV. We will thus represent the different vacua in the form

$$\{w_1, w_2, w_3\} = \{v_1, v_2 e^{i\theta_2}, v_3 e^{i\theta_3}\}. \tag{2.2}$$

[4]Let the indices $\{i, j, k\}$ be some permutation of $\{1, 2, 3\}$, and consider the vanishing of λ_i: The minimization conditions will then enforce the vanishing of λ_j and λ_k, unless the angles take on special values. Whenever all λ_l's vanish $V_{\rm ph}$ also vanishes and all VEVs can be made real.

It is convenient to extract an overall phase factor and decompose the SU(2) doublets as

$$\phi_i = e^{i\theta_i} \begin{pmatrix} \phi_i^+ \\ (v_i + \eta_i + i\chi_i)/\sqrt{2} \end{pmatrix}, \qquad i = 1, 2, 3. \tag{2.3}$$

In our convention, $\theta_1 = 0$, ϕ_1 being a reference for the phases of the other fields.

In general, *CP* is violated, so we cannot assign *CP* parities to the fields η_i and χ_i. However, since they are independent fields, they have opposite "*CP* content" in the sense that the product $\eta_i \chi_i$ is odd under *CP*.

The minimization with respect to the moduli of the VEVs gives

$$m_{11} = \lambda_{11} v_1^2 + \frac{1}{2}\bar{\lambda}_{12} v_2^2 + \frac{1}{2}\bar{\lambda}_{13} v_3^2 + \lambda_2 \cos(2\theta_3) v_3^2 + \lambda_3 \cos(2\theta_2) v_2^2, \tag{2.4a}$$

$$m_{22} = \lambda_{22} v_2^2 + \frac{1}{2}\bar{\lambda}_{12} v_1^2 + \frac{1}{2}\bar{\lambda}_{23} v_3^2 + \lambda_1 \cos(2\theta_3 - 2\theta_2) v_3^2 + \lambda_3 \cos(2\theta_2) v_1^2, \tag{2.4b}$$

$$m_{33} = \lambda_{33} v_3^2 + \frac{1}{2}\bar{\lambda}_{13} v_1^2 + \frac{1}{2}\bar{\lambda}_{23} v_2^2 + \lambda_1 \cos(2\theta_3 - 2\theta_2) v_2^2 + \lambda_2 \cos(2\theta_3) v_1^2, \tag{2.4c}$$

where we introduced the abbreviations

$$\bar{\lambda}_{12} \equiv \lambda_{12} + \lambda'_{12}, \qquad \bar{\lambda}_{13} \equiv \lambda_{13} + \lambda'_{13}, \qquad \bar{\lambda}_{23} \equiv \lambda_{23} + \lambda'_{23}. \tag{2.5}$$

These abbreviations are also useful for the neutral-sector mass matrices.

There are two minimization constraints with respect to the phases. These can be expressed as

$$\lambda_1 v_3^2 \sin(2\theta_2 - 2\theta_3) + \lambda_3 v_1^2 \sin 2\theta_2 = 0, \tag{2.6a}$$

$$\lambda_1 v_2^2 \sin(2\theta_3 - 2\theta_2) + \lambda_2 v_1^2 \sin 2\theta_3 = 0. \tag{2.6b}$$

From these two relations, it follows that the two phases are related via

$$\lambda_3 v_2^2 \sin 2\theta_2 + \lambda_2 v_3^2 \sin 2\theta_3 = 0. \tag{2.7}$$

It also follows that the relative sign of $\sin 2\theta_2$ and $\sin 2\theta_3$ is the opposite of the relative sign between λ_2 and λ_3.[5]

One can impose these two conditions (2.6) by substituting for λ_2 and λ_3,

[5]The ranges of these parameters could accordingly be reduced.

$$\lambda_2 = \frac{\lambda_1 v_2^2 \sin(2\theta_2 - 2\theta_3)}{v_1^2 \sin 2\theta_3}, \tag{2.8a}$$

$$\lambda_3 = -\frac{\lambda_1 v_3^2 \sin(2\theta_2 - 2\theta_3)}{v_1^2 \sin 2\theta_2}. \tag{2.8b}$$

Insisting on perturbativity, we require all $\lambda_i \in [-4\pi, 4\pi]$. Thus, whenever θ_2 or θ_3 is small, the other angle must be close (modulo $\pi/2$).

Alternatively, the minimization conditions (2.6) yield the solutions [6][6]

$$\cos 2\theta_2 = \frac{1}{2}\left[\frac{D_{23}D_{31}}{D_{12}^2} - \frac{D_{31}}{D_{23}} - \frac{D_{23}}{D_{31}}\right], \tag{2.9a}$$

$$\cos 2\theta_3 = \frac{1}{2}\left[\frac{D_{23}D_{12}}{D_{31}^2} - \frac{D_{12}}{D_{23}} - \frac{D_{23}}{D_{12}}\right], \tag{2.9b}$$

with

$$D_{12} = \lambda_3 (v_1 v_2)^2, \qquad D_{23} = \lambda_1 (v_2 v_3)^2,$$
$$D_{31} = \lambda_2 (v_3 v_1)^2. \tag{2.10}$$

Interpreting the D_{ij} as sides in a triangle [6] requires λ_1, λ_2, and λ_3 to all be positive. As noted above, θ_2 and θ_3 must then have opposite signs.

B. The case $\theta_2 = \theta_3 + n\pi/2$

When θ_2 and θ_3 differ by a multiple of $\pi/2$, the first terms of Eq. (2.6) vanish. These minimization conditions then require one of the following to be satisfied (assuming all VEVs are nonzero):

(1) $\lambda_2 = \lambda_3 = 0$,
(2) $\lambda_2 = 0$, $\sin 2\theta_2 = 0$,
(3) $\lambda_3 = 0$, $\sin 2\theta_3 = 0$, and
(4) $\sin 2\theta_2 = \sin 2\theta_3 = 0$.

All these cases are *CP* conserving and will not be considered in the following.

$\theta_2 = \theta_3$: When $\theta_2 = \theta_3$ we may go to a basis in which w_2 and w_3 are real, and w_1 is complex. It then follows that we have only one minimization condition with respect to phases; there will remain a "leftover" field on which the mass-squared matrix does not depend, i.e., a massless state.

$\theta_2 = \theta_3 \pm \pi$: This case is essentially equivalent to the case above, except for some sign changes.

$\theta_2 = \theta_3 \pm \pi/2$: This case is also essentially equivalent to the case above, except for an interchange of the η_i and χ_i fields in one doublet.

[6]These expressions differ from those of Ref. [6] since we take ϕ_1 rather than ϕ_2 to have a real VEV.

C. Rotating to a Higgs basis

To make these mass-squared matrices as simple as possible and to easily identify the SM Higgs in the neutral mass spectrum [cf. Eq. (5.1) below], it is convenient to rotate the Higgs doublets to a Higgs basis, where only one doublet has a nonzero VEV.

A suitable Higgs basis is reached by the transformation

$$\mathcal{R}_2 \mathcal{R}_1 \begin{pmatrix} v_1 \\ e^{i\theta_2} v_2 \\ e^{i\theta_3} v_3 \end{pmatrix} = \begin{pmatrix} v \\ 0 \\ 0 \end{pmatrix}, \tag{2.11}$$

with

$$\mathcal{R}_1 = \begin{pmatrix} 1 & 0 \\ 0 & R_1 \end{pmatrix}, \qquad R_1 = \frac{1}{w}\begin{pmatrix} v_2 e^{-i\theta_2} & v_3 e^{-i\theta_3} \\ -v_3 e^{-i\theta_2} & v_2 e^{-i\theta_3} \end{pmatrix},$$
$$w = \sqrt{v_2^2 + v_3^2}, \tag{2.12}$$

and

$$\mathcal{R}_2 = \frac{1}{v}\begin{pmatrix} v_1 & w & 0 \\ -w & v_1 & 0 \\ 0 & 0 & v \end{pmatrix}. \tag{2.13}$$

Thus, the Higgs basis [with SU(2) doublets H_1, H_2 and H_3] is reached by $\mathcal{R} \equiv \mathcal{R}_2 \mathcal{R}_1$,

$$\begin{pmatrix} H_1 \\ H_2 \\ H_3 \end{pmatrix} = \mathcal{R}\begin{pmatrix} \phi_1 \\ \phi_2 \\ \phi_3 \end{pmatrix} = \tilde{\mathcal{R}}\begin{pmatrix} \phi_1 \\ e^{-i\theta_2}\phi_2 \\ e^{-i\theta_3}\phi_3 \end{pmatrix}, \tag{2.14}$$

with

$$\tilde{\mathcal{R}} = \mathcal{R}_2 \frac{1}{w}\begin{pmatrix} w & 0 & 0 \\ 0 & v_2 & v_3 \\ 0 & -v_3 & v_2 \end{pmatrix} \tag{2.15}$$

in fact real.

We decompose the Higgs-basis fields as

$$H_1 = \begin{pmatrix} G^+ \\ (v + \eta_1^{\mathrm{HB}} + iG_0)/\sqrt{2} \end{pmatrix},$$
$$H_i = \begin{pmatrix} \varphi_i^{\mathrm{HB}+} \\ (\eta_i^{\mathrm{HB}} + i\chi_i^{\mathrm{HB}})/\sqrt{2} \end{pmatrix}, \qquad i = 2, 3, \tag{2.16}$$

and enumerate the neutral fields $\{1, 2, 3, 4, 5\}$ according to the following sequence:

$$\varphi_i^{\mathrm{HB}} = \{\eta_1^{\mathrm{HB}}, \eta_2^{\mathrm{HB}}, \eta_3^{\mathrm{HB}}, \chi_2^{\mathrm{HB}}, \chi_3^{\mathrm{HB}}\}, \quad i = 1, \ldots 5. \tag{2.17}$$

D. Masses

The elements of the 2×2 charged mass-squared matrix $\mathcal{M}^2_{\rm ch}$, as well as the masses squared, are given in Appendix A 1, while the elements of the 5×5 neutral mass-squared matrix $\mathcal{M}^2_{\rm neut}$ are given in Appendix A 2. Moreover, we give $\mathcal{O}(\lambda_1)$ formulas for the masses squared of the pseudo-Goldstone bosons in Appendix A 2 a.

We diagonalize the general neutral mass-squared matrix by a 5×5 rotation matrix O to obtain the mass eigenstates,

$$h_i = O_{ij}\varphi_j^{\rm HB}, \tag{2.18}$$

with $\varphi_j^{\rm HB}$ defined by Eq. (2.17).

Since the mass-squared matrix of the neutral sector is 5×5, the rotation matrix O of Eq. (2.18) can only be numerically determined. This somewhat limits our analysis. In Appendix A 2 we schematically quote the determinant (A8) of the neutral-sector mass-squared matrix. It is proportional to λ_1^2, reflecting the fact that the potential has two massless states in the limit $\lambda_1 \to 0$.

In Appendix B we briefly discuss a "minimal" version of the potential, with $\lambda_3 = \pm\lambda_2$, $\theta_3 = \mp\,\theta_2$, and $v_3 = v_2$. The mass-squared matrix of the neutral sector factorizes in that case, each factor vanishing linearly with λ_1. This suggests that these factors are related to the pseudo-Goldstone bosons.

1. Special cases

As shown in Appendix A 2, the mass-squared matrix for the neutral sector has the structure

$$\mathcal{M}^2_{\rm neut} = \begin{pmatrix} X & X & X & 0 & 0\\ X & X & X & 0 & x\\ X & X & X & x & 0\\ 0 & 0 & x & x & x\\ 0 & x & 0 & x & x \end{pmatrix} \begin{vmatrix} \eta_1^{\rm HB}\\ \eta_2^{\rm HB}\\ \eta_3^{\rm HB}\\ \chi_2^{\rm HB}\\ \chi_3^{\rm HB} \end{vmatrix}, \tag{2.19}$$

where elements that vanish as $\lambda_1 \to 0$ are denoted by lowercase x. The column to the right is a reminder of the field sequence in the Higgs basis. If we put $\sin(2\theta_2 - 2\theta_3) = 0$ we get a block-diagonal form with one massless state

$$\mathcal{M}^2_{\rm neut} = \begin{pmatrix} X & X & X & 0 & 0\\ X & X & X & 0 & 0\\ X & X & X & 0 & 0\\ 0 & 0 & 0 & 0 & 0\\ 0 & 0 & 0 & 0 & x \end{pmatrix} \begin{vmatrix} \eta_1^{\rm HB}\\ \eta_2^{\rm HB}\\ \eta_3^{\rm HB}\\ \chi_2^{\rm HB}\\ \chi_3^{\rm HB} \end{vmatrix}. \tag{2.20}$$

The condition $\lambda_1 = 0$ [instead of $\sin(2\theta_2 - 2\theta_3) = 0$] gives the above texture, only with a vanishing element on the last row and column ($x \to 0$), yielding a block-diagonal form with *two* massless *CP*-odd states.

Finally, for the "simple model" of Appendix B we have

$$\mathcal{M}^2_{\rm neut} = \begin{pmatrix} X & X & 0 & 0 & 0\\ X & X & x & 0 & 0\\ 0 & x & x & 0 & 0\\ 0 & 0 & 0 & x & x\\ 0 & 0 & 0 & x & X \end{pmatrix} \begin{vmatrix} \eta_1^{\rm HB}\\ \eta_2^{\rm HB}\\ \chi_3^{\rm HB}\\ \chi_2^{\rm HB}\\ \eta_3^{\rm HB} \end{vmatrix}, \tag{2.21}$$

which is also block diagonal, having interchanged rows (and columns) 3 and 5, i.e., swapped $\eta_3^{\rm HB}$ and $\chi_3^{\rm HB}$.

III. GAUGE COUPLINGS

The gauge-scalar couplings are determined by the kinetic part of the Lagrangian,

$$\mathcal{L}_{\rm kin} = \sum_{i=1,2,3} (D_\mu \phi_i)^\dagger (D^\mu \phi_i). \tag{3.1}$$

For the cubic gauge-gauge-scalar part, we get

$$\mathcal{L}_{VVh} = \left(g m_W W_\mu^+ W^{\mu-} + \frac{g m_Z}{2\cos\theta_W} Z_\mu Z^\mu \right) \sum_{i=1}^{5} O_{i1} h_i, \tag{3.2}$$

with the rotation matrix O relating physical states to the fields of the Higgs basis, as defined by Eq. (2.18). For the SM-like state at 125.25 GeV, this coupling O_{i1} is severely constrained by the LHC measurements [23]. Its magnitude must be close to unity.

For the cubic gauge-scalar-scalar terms, we find

$$\mathcal{L}_{Vhh} = -\frac{g}{2\cos\theta_W} \sum_{i=1}^{5}\sum_{j=1}^{5} (O_{i2}O_{j4} + O_{i3}O_{j5}) (h_i \overleftrightarrow{\partial_\mu} h_j) Z^\mu + \frac{g}{2} \sum_{i=1}^{5}\sum_{j=1}^{2} \left[(iO_{ij+1} + O_{ij+3}) \sum_{k=1}^{2} U_{jk} (h_k^+ \overleftrightarrow{\partial_\mu} h_i) W^{\mu-} + \text{H.c.} \right]$$
$$+ \left(ieA^\mu + \frac{ig\cos 2\theta_W}{2\cos\theta_W} Z^\mu \right) \sum_{j=1}^{2} (h_j^+ \overleftrightarrow{\partial_\mu} h_j^-), \tag{3.3}$$

and for the quartic gauge-gauge-scalar-scalar terms, we find

$$\mathcal{L}_{VVhh} = \left(\frac{g^2}{4} W_\mu^+ W^{\mu-} + \frac{g^2}{8\cos^2\theta_W} Z_\mu Z^\mu\right) \sum_{i=1}^{5} h_i^2 + \left(\frac{g^2}{2} W_\mu^+ W^{\mu-} + e^2 A_\mu A^\mu + \frac{g^2 \cos^2 2\theta_W}{\cos^2\theta_W} Z_\mu Z^\mu + \frac{eg\cos 2\theta_W}{\cos\theta_W} A_\mu Z^\mu\right) \times \sum_{j=1}^{2} h_j^+ h_j^- + \left[\left(\frac{eg}{2} W_\mu^+ A^\mu - \frac{g^2 \sin^2\theta_W}{2\cos\theta_W} W_\mu^+ Z^\mu\right) \sum_{i=1}^{5} \sum_{j,k=1}^{2} U_{jk} h_i h_k^- \left(O_{ij+1} + i O_{ij+3}\right) + \text{H.c.}\right]. \tag{3.4}$$

We have argued that the vicinity of the $U(1) \times U(1)$ symmetry should have an impact on the scalar sector, leading to light states that when $\lambda_1 \to 0$ reveal their Goldstone origin and become odd under CP. In order to shed light on this, we will analyze the coupling of the Z boson to a pair of scalars. Since Z is odd under CP, it will only couple to the odd component of a two-scalar state $h_i h_j$, not the even part. This odd component attains its maximal value when one scalar is even and the other is odd.

A measure of the CP content of two states is obtained from the trilinear coupling $h_i h_j Z$. From the first line of Eq. (3.3), an obvious measure is

$$P_{ij} = (O_{i2} O_{j4} + O_{i3} O_{j5}) - (i \leftrightarrow j). \tag{3.5}$$

We shall refer to it as the "Z affinity" of a pair of scalars. A high affinity would mean that the $h_i h_j$ two-scalar state has a significant CP-odd component. Since a two-particle state consisting of two even or two odd scalars would be CP even, we shall somewhat imprecisely refer to the above situation of a large $|P_{ij}|$ as saying the two states have different CP profiles. The quantity P_{ij} is basis independent, since it refers to a coupling among physical states.

As a reference, it is worth analyzing the Z affinities of pairs of scalars in the CP-conserving 2HDM. We adopt the conventional terminology of h and H being even under CP, whereas A is odd. Furthermore, we take h to be the SM state at 125 GeV. One readily finds that the Z affinity of h and H (both CP even) is zero, whereas that of H and A is unity. However, by the above definition and in the limit of alignment, the Z affinity of h and A is also zero. With $h = h_j$ aligned, we have $O_{j1} = 1$, and (by orthogonality) $O_{k1} = O_{jk} = 0$, with $k \neq j$. Thus, when h_j is aligned, then $P_{kj} = P_{jk} = 0$ for all k.

Whereas in the 2HDM, allowing for CP violation, the $h_i h_j Z$ couplings are essentially the same as the $h_k ZZ$ couplings [24], with i, j, k all different, this is not the case in a 3HDM.

Since $P_{ij} = -P_{ji}$ and $P_{ii} = 0$, it follows that there are ten quantities, matching the fact that the rotation matrix O can be generated by ten independent angles. Invoking the orthogonality of the rotation matrix, as well as the five independent $h_i VV$ couplings O_{i1}, it has been shown that there are, in fact, only seven independent couplings [25].[7] We do, however, find it more transparent to work within this set of ten quantities (3.5), but note from the 2HDM example given above that different CP does not necessarily yield a high value for $|P_{ij}|$. However, a high value for $|P_{ij}|$ can only emerge from states having different CP content.

One may extend the usefulness of the measure of relative CP of two states into the region of small, but nonzero O_{j1} by normalizing it to the squared sum of even and odd couplings,

$$\hat{P}_{ij} = \frac{P_{ij}}{\sqrt{\min(O_{i1}^2, O_{j1}^2) + P_{ij}^2}}, \tag{3.6}$$

with O_{i1} representing the CP-even part of the ZZh_i coupling. This measure enhances the affinity in parameter regions where it would otherwise be small, due to near alignment.[8]

A measure of the CP-odd content of a state can be obtained by summing the square of this coupling over all the other states, $j \neq i$. We denote the square of this quantity $\tilde{P}_i^2$,

$$\tilde{P}_i^2 = \sum_{j \neq i} P_{ij}^2 = \sum_{j} P_{ij}^2 = \sum_{j \neq i} O_{j1}^2 = 1 - O_{i1}^2, \tag{3.7}$$

where in the second step we have used the fact that $P_{ii} = 0$ and, in the following, the orthogonality of O. This has a straightforward interpretation: While we may think of $|O_{i1}|$ as a measure of the CP-even content of h_i, we may think of

$$\tilde{P}_i = \sqrt{1 - O_{i1}^2} \tag{3.8}$$

as the CP-odd part.

IV. YUKAWA COUPLINGS

With complex VEVs, there will also be CP violation in the Yukawa sector, even with real Yukawa couplings. The actual amount of CP violation will depend on how the

[7]This mismatch between the ten underlying rotation angles and the seven independent couplings is due to the fact that some sets of rotation angles $(\alpha_{12}, \alpha_{13}, \ldots, \alpha_{45})$ and $(\alpha'_{12}, \alpha'_{13}, \ldots, \alpha'_{45})$ yield the *same* rotation matrix O.

[8]This normalization would fail in the zero-measure limit of both h_i and h_j being purely CP odd, i.e., having $\min(O_{i1}, O_{j1}) = 0$ *and* $P_{ij} = 0$.

SU(2) doublets couple to the fermions. As an example, we shall consider natural flavor conservation, where each fermion species couples to at most one Higgs doublet [2]. One way to implement this is to let each right-handed fermion sector u, d, and e couple to a different Higgs doublet according to the following $\mathbb{Z}_2 \times \mathbb{Z}_2$ charges:

$$\phi_1:(+1,+1) \qquad \phi_2:(-1,+1) \qquad \phi_3:(+1,-1), \tag{4.1a}$$

$$u_R:(+1,+1) \qquad d_R:(-1,+1) \qquad e_R:(+1,-1). \tag{4.1b}$$

Then the Yukawa Lagrangian takes the form

$$\mathcal{L}_Y = \bar{Q}_L Y^u \tilde{\phi}_1 u_R + \bar{Q}_L Y^d \phi_2 d_R + \bar{E}_L Y^e \phi_3 e_R + \text{H.c.} \tag{4.2}$$

Expanding the doublets and rewriting the Yukawa neutral interactions in terms of the physical fermion fields, we obtain, in addition to mass terms,

$$\mathcal{L}_Y^{\text{neutral}} = \frac{1}{v_1}\bar{u}M^u(\eta_1 + i\chi_1\gamma_5)u + \frac{1}{v_2}\bar{d}M^d(\eta_2 + i\chi_2\gamma_5)d + \frac{1}{v_3}\bar{e}M^e(\eta_3 + i\chi_3\gamma_5)e. \tag{4.3}$$

Mixing between the η_i and χ_i fields will cause the neutral physical scalars to have CP-violating interactions with the fermions. The Yukawa interaction between a neutral physical scalar h_i and a fermion f takes the general form

$$\mathcal{L}_{h_i ff} = \frac{m_f}{v} h_i \left(\kappa^{h_i ff}\bar{f}f + i\tilde{\kappa}^{h_i ff}\bar{f}\gamma_5 f\right). \tag{4.4}$$

This structure can be used to quantify the CP content of the physical scalars. For the case of $\tau\bar{\tau}$ final states, CMS [26] has measured this mixing, defined through

$$\tan\alpha^{h_{\text{SM}}\tau\tau} = \frac{\tilde{\kappa}^{h_{\text{SM}}\tau\tau}}{\kappa^{h_{\text{SM}}\tau\tau}}. \tag{4.5}$$

It has also been suggested to try to measure this quantity for the 2HDM [27].

In order to identify this quantity, we need to express the fields η_i and χ_i of Eq. (4.3) in terms of the physical scalars, which are not eigenstates of CP. For this purpose, we start by "undoing" the transformation to the Higgs basis (2.14), writing the inverse, for the neutral fields, in the form

$$\begin{pmatrix} \eta_1 + i\chi_1 \\ \eta_2 + i\chi_2 \\ \eta_3 + i\chi_3 \end{pmatrix} = \tilde{\mathcal{R}}^T \begin{pmatrix} \eta_1^{\text{HB}} + iG^0 \\ \eta_2^{\text{HB}} + i\chi_2^{\text{HB}} \\ \eta_3^{\text{HB}} + i\chi_3^{\text{HB}} \end{pmatrix}, \tag{4.6}$$

with $\tilde{\mathcal{R}}$ given by Eq. (2.15). Next, the η_i^{HB} and χ_i^{HB}, collectively referred to as φ_i^{HB} according to Eq. (2.17), can be expressed in terms of the physical states h_i via Eq. (2.18).

If we introduce a complex quantity for the couplings to ϕ_k according to Eq. (4.3),

$$\begin{aligned} Z_i^{(k)} &= \left(\tilde{\mathcal{R}}^T\right)_{k1} O_{i1} + \left(\tilde{\mathcal{R}}^T\right)_{k2}(O_{i2} + iO_{i4}) \\ &\quad + \left(\tilde{\mathcal{R}}^T\right)_{k3}(O_{i3} + iO_{i5}) \\ &= \tilde{\mathcal{R}}_{1k}O_{i1} + \tilde{\mathcal{R}}_{2k}(O_{i2} + iO_{i4}) + \tilde{\mathcal{R}}_{3k}(O_{i3} + iO_{i5}), \end{aligned} \tag{4.7}$$

then for the coupling of h_i to $\tau\bar{\tau}$ ($k = 3$), we have

$$\kappa^{h_i ee} = \frac{v}{v_3}\text{Re}Z_i^{(3)}, \qquad \tilde{\kappa}^{h_i ee} = \frac{v}{v_3}\text{Im}Z_i^{(3)}, \tag{4.8}$$

and

$$\alpha^{h_i\tau\tau} = \arg\left(Z_i^{(3)}\right). \tag{4.9}$$

Some quantitative comments on this quantity will be presented in Sec. VI C.

As pointed out in the Introduction, this model cannot generate a complex CKM matrix and therefore cannot be considered as the full description.

V. PARAMETER SCANS OF THE SCALAR POTENTIAL

The fact that LHC experiments have determined the Higgs-gauge coupling $h_{\text{SM}}WW$ to be very close to the SM value shows that the observed Higgs state is essentially pure scalar, with no or very little pseudoscalar admixture. In the notation of Eq. (3.2), this means that

$$|O_{j1}| \simeq 1, \qquad \text{for some } j. \tag{5.1}$$

We have performed scans over parameters, analyzing the mass spectrum and imposing a condition on the coupling of the SM-like state to two gauge bosons. Each parameter point is required to satisfy boundedness from below, perturbativity, and tree-level unitarity. For boundedness from below, only sufficient conditions are known for the $\mathbb{Z}_2 \times \mathbb{Z}_2$-symmetric potential [28,29] and we therefore opt for a numerical check, whereas conditions for tree-level unitarity conditions are taken from [30]. We uniformly sample the parameters in the largest region where all the above constraints can be met[9]

[9]Alternatively, the scan could be "factorized" into a scan over the parameters determining the neutral sector, replacing λ_{ij} and λ'_{ij} by $\bar{\lambda}_{ij}$, and another over the charged sector. Qualitatively, the results are found to be similar.

TABLE I. Distribution (in percentage) of h_j with gauge coupling h_jWW in agreement with the SM, within 3σ.

	h_1	h_2	h_3	h_4	h_5
PDG [23]	0.31	38.23	28.00	22.51	10.95
ATLAS [31]	0.31	38.53	27.12	21.19	12.85
With theoretical cuts	0.01	27.88	30.69	27.68	13.74

$$v_i \in [0, v], \qquad i = 1,2,3, \text{ with } v_1^2 + v_2^2 + v_3^2 = v^2, \tag{5.2a}$$

$$\theta_i \in [-\pi, \pi], \qquad i = 2,3, \tag{5.2b}$$

$$\lambda_{ii} \in [0, 4\pi], \qquad i = 1,2,3, \tag{5.2c}$$

$$\lambda_{ij}, \lambda'_{ij} \in [-4\pi, 4\pi], \quad i,j = 1,2,3, \tag{5.2d}$$

$$\lambda_1 \in [-4\pi, 4\pi]. \tag{5.2e}$$

From these parameters one can reconstruct the mass-squared matrices and diagonalize them. The neutral mass eigenvalues are ordered as

$$m_1 < m_2 < m_3 < m_4 < m_5. \tag{5.3}$$

Since the mass-squared matrix is homogeneous in the λ's, we can rescale the λ's (all by the same factor) and thereby rescale the masses. The analysis of the sampled parameter points is performed as follows. For each $j = 1$ to 5:

(1) check that the coupling O_{j1} of h_j to WW (or ZZ) is compatible with LHC measurements [23] (at most one value of j will be accepted),
(2) rescale all λ's such that $m_j = m_{\rm SM} = 125.25$ GeV,
(3) apply theoretical cuts (boundedness from below, perturbativity, and tree-level unitarity) on all rescaled λ's (including λ_2 and λ_3), and
(4) check that the lightest charged scalar is above 80 GeV.

If these conditions are satisfied, the parameter point is kept. Regarding the LHC measurements of the Higgs-gauge couplings hVV ($V = W, Z$), we use the ATLAS run 2 value for the coupling modifier κ_V [23] with a 3σ tolerance, resulting in the following constraint for the SM-like state:

$$|O_{j1}| > 0.93. \tag{5.4}$$

Thus, we obtain the h_j distribution given in Table I. The theoretical constraints referred to under point 3 are boundedness from below (within the limitation specified above), perturbativity, and unitarity. We note that if these essential experimental and theoretical constraints are to be satisfied then the scenario where h_1 is the SM-like state requires fine-tuning of the parameters.

We observe that small values of λ_i are required to satisfy all the constraints. This is illustrated by Fig. 1, where it is seen that the distribution of λ_1 becomes narrower as the constraint on the h_iVV coupling is applied. The further constraints from boundedness from below and unitarity (right-hand panel) have only a modest impact. These histograms can be characterized by their rms values:

$$\lambda_1|_{\rm unconstrained} = 1.91, \qquad \lambda_1|_{3\sigma} = 0.66, \qquad \lambda_1|_{3\sigma+\text{th cuts}} = 0.37. \tag{5.5}$$

Thus, when the constraint on the h_iVV coupling is imposed, this potential has an approximate $U(1) \times U(1)$ symmetry in a sizable fraction of its viable parameter space.

The parameter points have also been analyzed in terms of the average (rms) P_{ij}, representing the coupling of two

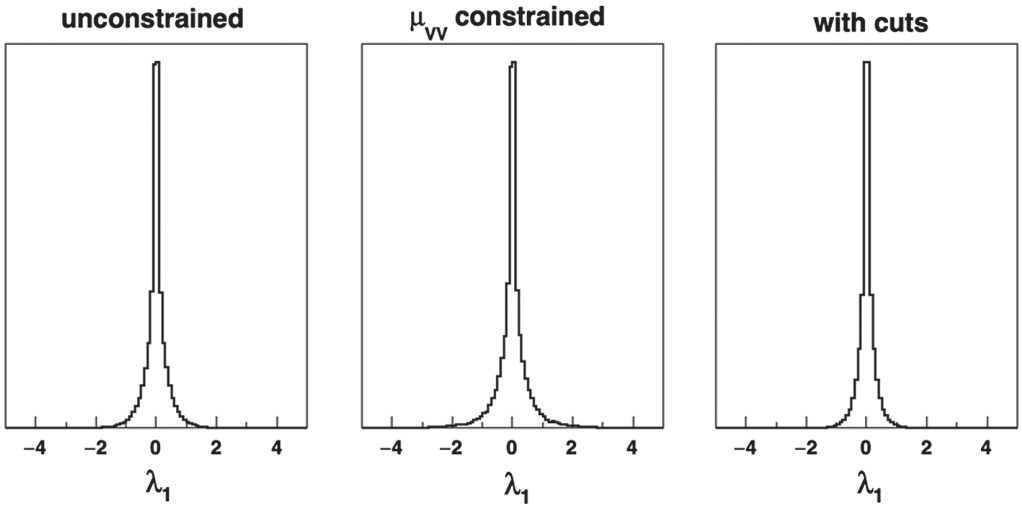

FIG. 1. Histograms of λ_1 without (left) and with (center and right) the constraint $|(O_{j1})^2 - \kappa_V^2| < n\sigma$ with $n = 3$. On the right, we show the impact of imposing further theory constraints (see text).

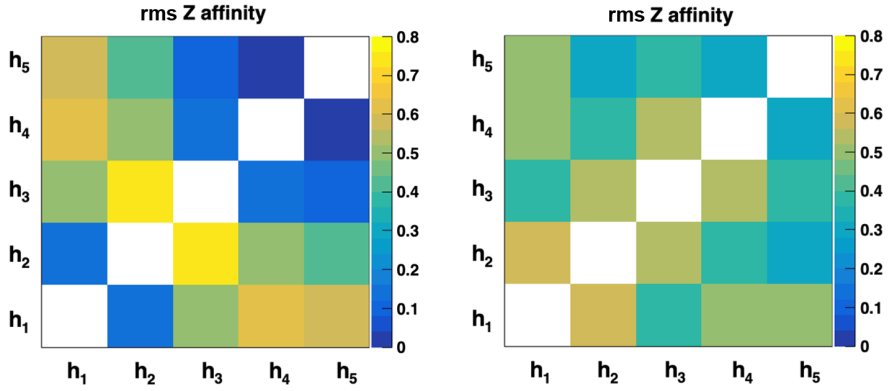

FIG. 2. Average Z affinity $(P_{ij})_{\text{rms}}$ of states h_i and h_j. Left: the $U(1) \times U(1)$ limit, as defined by Eq. (5.6). Right: no restriction on the λ's.

neutral scalars to the Z boson, defined by Eq. (3.5). We interpret this as a measure of their relative CP. We have also studied the absolute CP-odd content, as defined by Eq. (3.8). If the average (rms) P_{ij} is large, we say their CP content is different (even if the absolute $\tilde{P}_i$ and $\tilde{P}_j$ might be similar), whereas if it is small, we shall say that their CP content is similar.

For this study, as a reference, we also analyzed parameter points that were not subject to the experimental SM-like Higgs constraints described above. In Fig. 2 we compare rms Z affinities for all pairs of neutral scalars and for two cases, both without the SM-like constraint. In the left panel, we impose a "near $U(1) \times U(1)$ symmetry" condition

$$\max(|\lambda_1|, |\lambda_2|, |\lambda_3|) = 0.01, \tag{5.6}$$

whereas in the right panel we impose no such constraint, i.e., we do not restrict the scan to the regime of near $U(1) \times U(1)$ symmetry. The left panel shows a clear separation into two sets of states, h_1 and h_2 have low affinity to the Z, meaning they have similar CP content, as does the other set, h_3, h_4, and h_5. It is natural to interpret this as follows: Near the $U(1) \times U(1)$ limit, we have two neutral states that are approximately odd under CP and three that are approximately even. This is fully in accord with the expectations from the Goldstone theorem [32,33], since the Goldstone bosons in the $U(1) \times U(1)$ limit will be CP odd [34].

It is instructive to consider how the Z affinity is affected by alignment. Let h_j be "aligned," meaning its coupling to WW is maximal, $O_{j1} = 1$. By orthogonality, it follows that $O_{k1} = 0$ for $k \neq j$ and $O_{jk} = 0$ for $k \neq 1$. Then,

$$P_{ij} = P_{ji} = 0 \quad \text{for all } i, \tag{5.7}$$

the aligned scalar h_j has no Z affinity with any other h_i [34]. This is analogous to the CP-even and aligned (and SM-like) h in a CP-conserving 2HDM not having any Z affinity to the pseudoscalar A, even though they have opposite CP.

The features displayed in Fig. 2 change when we turn on the SM-like constraint. We shall next consider h_2 and h_3 as candidates for being the discovered state at 125.25 GeV.

VI. ACCOMMODATING AN SM-LIKE STATE h_{SM}

Assuming h_2 or h_3 is identified as h_{SM}, we shall here first discuss the CP profiles of the light states, as determined from the gauge couplings, and then subsequently study the Yukawa couplings.

A. h_2 as h_{SM}

We first consider the possibility that h_2 is to be identified with the discovered SM-like state at 125.25 GeV, as suggested by Table I.

For the parameter points that survive the constraints, we show in Fig. 3 the distributions of the complex VEVs $v_2 e^{i\theta_2}$ and $v_3 e^{i\theta_3}$. Superimposed on circular structures with "holes" at $v_2 = 0$ and $v_3 = 0$, there are depressions at purely real and purely imaginary values. The latter are due to the fact that λ_2 and/or λ_3 become nonperturbative when $|\sin 2\theta_2|$ or $|\sin 2\theta_3|$ are small.

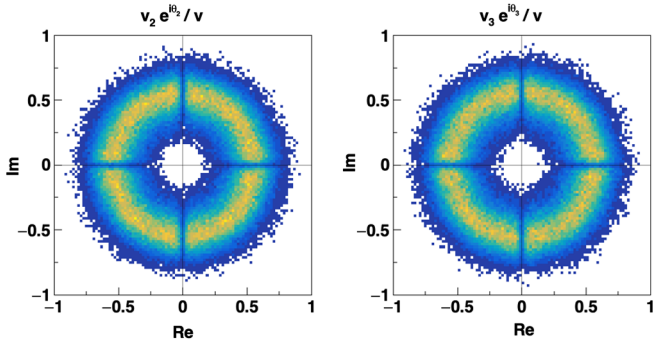

FIG. 3. Scatter plots of real and imaginary parts of the complex VEVs $v_2 e^{i\theta_2}/v$ (left) and $v_3 e^{i\theta_3}/v$ (right), for $h_2 = h_{\text{SM}}$. The number of surviving parameter points increases when going from dark blue to yellow.

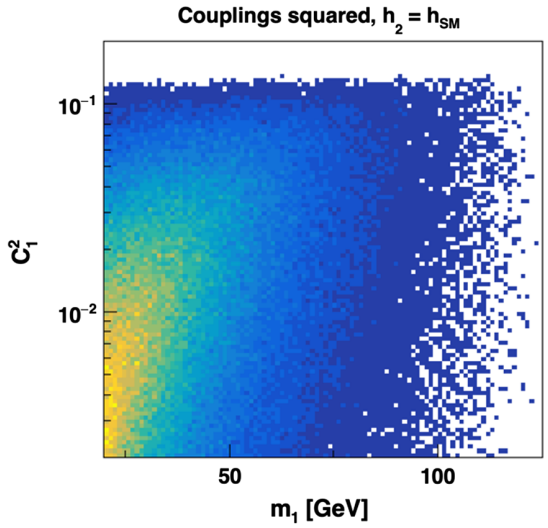

FIG. 4. Distributions of squared gauge couplings C_1^2 of h_1 vs mass (arbitrary units, with yellow "high" and dark blue "low").

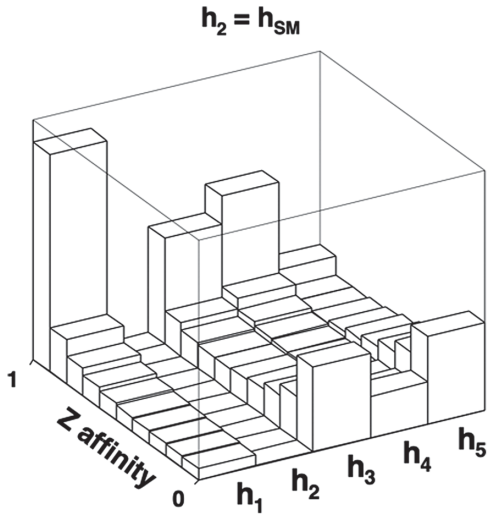

FIG. 5. Frequency distribution of the relative strength $|\hat{P}_{2j}|$ of the h_2h_jZ couplings, in units of $g/(2\cos\theta_W)$ (along the y axis) vs h_j.

If h_2 were the discovered Higgs particle at 125.25 GeV, why has h_1 escaped detection? Searches at LEP [35,36] depend on production via the Bjorken mechanism, where the hZZ coupling is essential. But within the present scenario, the h_1ZZ coupling O_{11} is suppressed. This is illustrated in Fig. 4, where we plot

$$C_1^2 \equiv |O_{11}|^2 \tag{6.1}$$

vs m_1. The bulk of the scan points lie at masses below 50 GeV and for a squared coupling of the order 10^{-2}. This suppression is simply a result of the unitarity of the mixing matrix O.

It is interesting to examine the profile of the neutral state h_1 that in this scenario is lighter than 125 GeV. Is it related to the breaking of the $U(1)$ symmetries discussed in the Introduction? In particular, does it have a significant CP-odd content? Since the gauge field Z is odd under CP, we can ask how large the h_1h_2Z coupling is, recalling that, in the familiar CP-conserving 2HDM, there is an HAZ coupling of strength 1 [in units of $g/(2\cos\theta_W)$]. The corresponding coupling is for the Weinberg potential given by Eq. (3.6), from the first term of Eq. (3.3). We show in Fig. 5 the distribution of the h_2h_jZ couplings, in the above units. The strongest coupling is seen to be to $h_j = h_1$, consistent with it having a sizable CP-odd component.

B. h_3 as $h_{\rm SM}$

We next assume that h_3 is to be identified as the discovered SM-like scalar.

For the parameter points that survive the above constraints on maximal allowed value of the $|\lambda|$'s and minimum allowed charged Higgs mass, we show in Fig. 6 the distributions of the complex VEVs $v_2e^{i\theta_2}$ and $v_3e^{i\theta_3}$. As compared with the previous case, $h_2 = h_{\rm SM}$, the small-v_2 and small-v_3 regions are here less depleted.

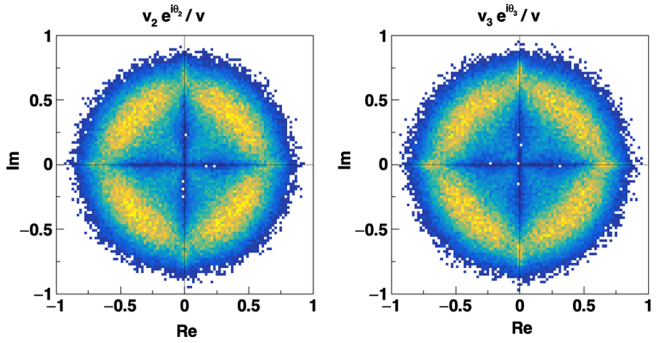

FIG. 6. Scatter plots of real and imaginary parts of the complex VEVs $v_2e^{i\theta_2}/v$ (left) and $v_3e^{i\theta_3}/v$ (right) for $h_3 = h_{\rm SM}$. Yellow is high, dark blue is low.

In analogy with the case above, we examine the profile of the neutral states h_1 and h_2 that in this scenario are lighter than 125 GeV and show in Fig. 7 the distribution of h_3h_jZ couplings. The strongest coupling is again seen to be to $h_j = h_1$.

C. Yukawa couplings

Returning now to the Yukawa couplings, we study the angle α, which is a measure of the relative CP-odd component of this coupling. In Fig. 8 we show scatter plots[10] of α (in units of its maximum value, $\pi/2$) for the five different neutral states in the two scenarios $h_2 = h_{\rm SM}$ and $h_3 = h_{\rm SM}$. In both cases $h_{\rm SM}$ is subject to the constraint $|\alpha| < 0.1$, which ensures that the CP-odd part of the

[10]For better visibility, the points are randomly distributed along the horizontal dimension.

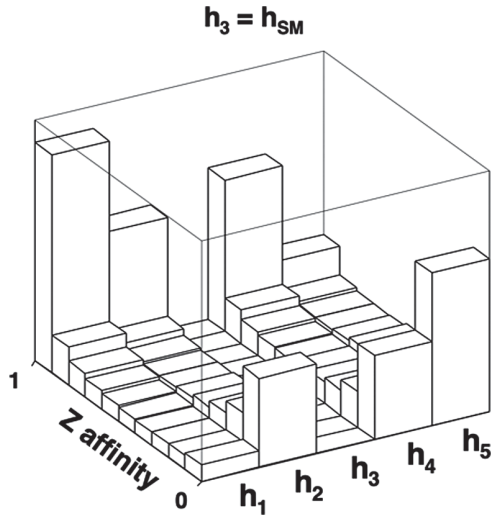

FIG. 7. Frequency distribution of the relative strength $|\hat{P}_{3j}|$ of the $h_3 h_j Z$ couplings, in units of $g/(2\cos\theta_W)$ (along the y axis) vs h_j.

Yukawa coupling $h_{\rm SM}\bar{\tau}\tau$ is consistent with experimental measurements [26].

This figure supports the feature of the Weinberg potential presented in the Introduction: in each scenario, the states lighter than $h_{\rm SM}$ are more likely to have a significant *CP*-odd content than the heavier ones.

It should be stressed that the results shown in Fig. 8 depend on how natural flavor conservation is implemented, cf. (4.1). Because of the symmetry (statistically speaking) of the potential under interchange of ϕ_i with ϕ_j, the scan result does not depend on whether the fermion in question (here, the τ) is coupled to ϕ_1, ϕ_2, or ϕ_3. What is important, though, is the fact that it is coupled to only *one* doublet. The outcome would be different if the assumption of natural flavor conservation were relaxed. If τ, e.g., couples to both ϕ_2 and ϕ_3, then the angle α would instead be given by

$$\alpha^{h_i\tau\tau} = \arg\left[\frac{v}{v_2}Z_i^{(2)} + \frac{v}{v_3}Z_i^{(3)}\right]. \tag{6.2}$$

VII. CONCLUSIONS

We have explored the spectrum of the Weinberg scalar potential with real coefficients in some detail, determining the *CP* profiles of the neutral states from how they couple to the electroweak gauge bosons and to fermions. We find that if this potential accommodates the discovered, approximately *CP*-even Higgs boson at 125.25 GeV, then it naturally (i.e., in the absence of fine-tuning) predicts one or two lighter neutral states. While the model violates *CP*, one of these states, or both, would have a significant *CP*-odd content.

One might wonder whether or not imposing the conditions listed in Sec. V in our parameter scan would bring us close to one of the symmetries obtained for natural alignment in Ref. [18]. This would require simple relations among the parameters of the potential [37,38]. We have checked that this is not the case. Therefore, the requirement of being close to alignment simply translates into an appropriate choice of parameter space.

In spite of some hints [35,36,39–42], no state with $m < 125$ GeV has been observed. This could simply be because in this model the $h_i ZZ$ coupling is for the lighter states typically below 10% of the SM value and production via the Bjorken process is suppressed.

In view of these results and the appeal of the Weinberg potential, it seems important to pursue the searches for a light scalar, whose coupling to the Z and W is reduced. In this context, it is important to recall that also branching

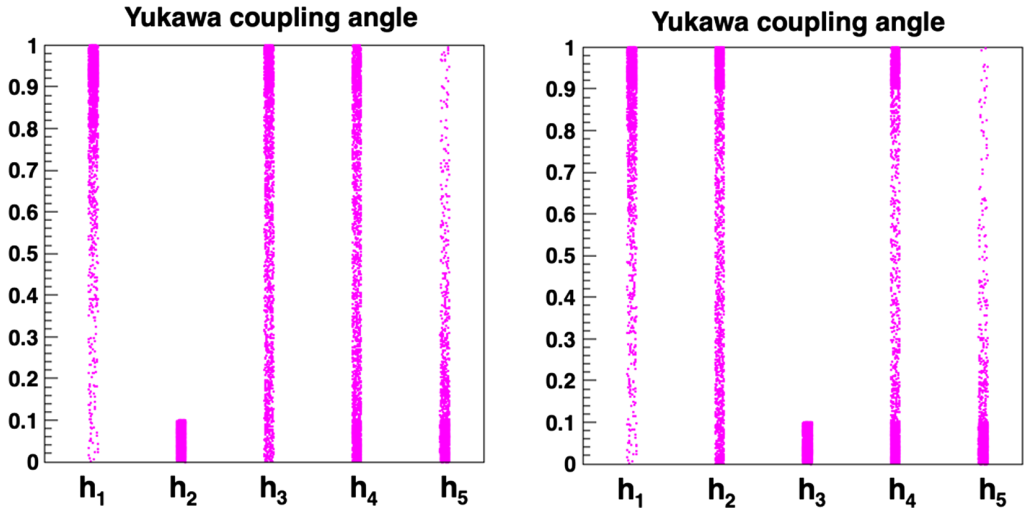

FIG. 8. Scatter plots of the absolute value of the angle α (in units of $\pi/2$) of Eq. (4.9), characterizing the *CP*-odd content of the Yukawa couplings to $\tau\bar{\tau}$ for $h_2 = h_{\rm SM}$ (left) and $h_3 = h_{\rm SM}$ (right).

ratios would differ from those of the SM Higgs. In particular, the $h_j \to \gamma\gamma$ rate would be reduced, again because of the reduced $h_i WW$ coupling and also modified by the loop contributions of the charged scalars. This issue will be discussed elsewhere; the contribution of the charged states could lead to either destructive or constructive interference with the W and fermion loops.

In Ref. [28] the same real scalar potential with an additional complex soft symmetry breaking term is studied in a region of parameter space such that the vacuum leaves one of the $\mathbb{Z}_2$ symmetries unbroken, i.e., one of the doublets acquires zero VEV. The additional soft term is introduced to explicitly break the two $\mathbb{Z}_2$ symmetries that are also broken by the vacuum. In this way it is possible to have CP violated explicitly by the potential. This framework results in a viable extension of the inert doublet model [43–45], providing a good dark matter candidate while having two noninert doublets.

ACKNOWLEDGMENTS

P. O. is supported in part by the Research Council of Norway. The work of M. N. R. was partially supported by Fundação para a Ciência e a Tecnologia (FCT, Portugal) through the projects CFTP-FCT Unit UIDB/00777/2020 and UIDP/00777/2020, PTDC/FIS-PAR/29436/2017, CERN/FIS-PAR/0008/2019, CERN/FIS-PAR/0002/2021, which are partially funded through Programa Operacional Ciência, Tecnologia, Inovação (POCTI) (Fundo Europeu de Desenvolvimento Regional (FEDER)), Programa Operacional Competitividade e Internacionalização (COMPETE), Quadro de Referência Estratégia Nacional (QREN), and European Union (EU). We also thank Centro de Física Teórica de Partículas/Instituto Superior Técnico/University of Lisbon and the University of Bergen, where collaboration visits took place.

APPENDIX A: THE MASS-SQUARED MATRICES

In this appendix, we give the mass-squared matrices of the Weinberg potential.

1. Charged sector

In the charged sector, the elements of the 2×2 mass-squared matrix corresponding to the fields $\varphi_2^{\mathrm{HB}\pm}$ and $\varphi_3^{\mathrm{HB}\pm}$ can be written as

$$(\mathcal{M}^2_{\mathrm{ch}})_{11} = -\frac{\lambda_1 v^2 \sin^2(2\theta_2 - 2\theta_3) v_2^2 v_3^2}{\sin 2\theta_2 \sin 2\theta_3 v_1^2 w^2} - \left(\lambda'_{12} v_2^2 + \lambda'_{13} v_3^2\right) \frac{v^2}{2w^2}, \tag{A1a}$$

$$(\mathcal{M}^2_{\mathrm{ch}})_{12} = -\frac{\lambda_1 v v_1 v_2 v_3 \sin(2\theta_2 - 2\theta_3)}{\sin 2\theta_2 \sin 2\theta_3 v_1^2 w^2} \times \left(v_2^2 \sin 2\theta_2 e^{2i\theta_3} + v_3^2 \sin 2\theta_3 e^{2i\theta_2}\right) + \frac{v v_1 v_2 v_3}{2w^2} \left(\lambda'_{12} - \lambda'_{13}\right), \tag{A1b}$$

$$(\mathcal{M}^2_{\mathrm{ch}})_{21} = (\mathcal{M}^2_{\mathrm{ch}})^*_{12}, \tag{A1c}$$

$$(\mathcal{M}^2_{\mathrm{ch}})_{22} = -\frac{\lambda_1}{\sin 2\theta_2 \sin 2\theta_3 w^2} \left(2 \sin 2\theta_2 \sin 2\theta_3 \times \cos(2\theta_2 - 2\theta_3) v_2^2 v_3^2 + \sin^2 2\theta_2 v_2^4 + \sin^2 2\theta_3 v_3^4\right) - \frac{1}{2w^2} \left[(\lambda'_{12} v_3^2 + \lambda'_{13} v_2^2) v_1^2 + \lambda'_{23} w^4\right]. \tag{A1d}$$

These are all singular if either θ_2 or θ_3 vanishes faster than the other one. The singularities arise due to the constraints (2.8).

For the rotation to the mass eigenstates $h^+_{1,2}$ we introduce a complex matrix U,

$$h_i^+ = U_{ij} \varphi_{j+1}^{\mathrm{HB}+}, \tag{A2}$$

with $\varphi_{2,3}^{\mathrm{HB}+}$ defined by Eq. (2.16). Explicitly, with

$$U = \begin{pmatrix} \cos\gamma & \sin\gamma e^{i\phi} \\ -\sin\gamma e^{-i\phi} & \cos\gamma \end{pmatrix}, \tag{A3}$$

we have $h_1^+ = \cos\gamma \varphi_2^{\mathrm{HB}+} + \sin\gamma e^{i\phi} \varphi_3^{\mathrm{HB}+}$ and $h_2^+ = -\sin\gamma e^{-i\phi} \varphi_2^{\mathrm{HB}+} + \cos\gamma \varphi_3^{\mathrm{HB}+}$.

The masses in the charged sector are thus given entirely in terms of λ_1, λ'_{12}, λ'_{13}, and λ'_{23}, together with the VEVs and the phases. The unprimed λ_{ij} do not enter. Furthermore, for small λ_1, either λ'_{12} and/or λ'_{13} and/or λ'_{23} must be negative.

2. Neutral sector

With the Higgs-basis field sequence (2.17) and invoking Eq. (2.8), we find

$$(\mathcal{M}^2_{\text{neut}})_{11} = \frac{4\lambda_1 v_2^2 v_3^2}{v^2 \sin 2\theta_2 \sin 2\theta_3}\left[1 - \cos(2\theta_2 - 2\theta_3)\cos 2\theta_2 \cos 2\theta_3\right] + \frac{2}{v^2}\left[\lambda_{11} v_1^4 + \lambda_{22} v_2^4 + \lambda_{33} v_3^4 + \bar{\lambda}_{12} v_1^2 v_2^2 + \bar{\lambda}_{13} v_1^2 v_3^2 + \bar{\lambda}_{23} v_2^2 v_3^2\right], \tag{A4a}$$

$$(\mathcal{M}^2_{\text{neut}})_{12} = \frac{-2\lambda_1 v_2^2 v_3^2}{v^2 w v_1 \sin 2\theta_2 \sin 2\theta_3}\left[\sin^2(2\theta_2 - 2\theta_3)(2w^2 - v^2) - 2\cos(2\theta_2 - 2\theta_3)\sin 2\theta_2 \sin 2\theta_3 v_1^2\right] - \frac{v_1}{v^2 w}\left[2\lambda_{11} v_1^2 w^2 - 2\lambda_{22} v_2^4 - 2\lambda_{33} v_3^4 - (\bar{\lambda}_{12} v_2^2 + \bar{\lambda}_{13} v_3^2)(v^2 - 2w^2) - 2\bar{\lambda}_{23} v_2^2 v_3^2\right], \tag{A4b}$$

$$(\mathcal{M}^2_{\text{neut}})_{13} = \frac{2\lambda_1 v_2 v_3}{vw \sin 2\theta_2 \sin 2\theta_3}\left[v_2^2 \sin^2 2\theta_2 - v_3^2 \sin^2 2\theta_3\right] + \frac{v_2 v_3 w}{vw^2}\left[-2\lambda_{22} v_2^2 + 2\lambda_{33} v_3^2 - \bar{\lambda}_{12} v_1^2 + \bar{\lambda}_{13} v_1^2 + \bar{\lambda}_{23}(v_2^2 - v_3^2)\right], \tag{A4c}$$

$$(\mathcal{M}^2_{\text{neut}})_{22} = \frac{4\lambda_1 v_2^2 v_3^2}{v^2 w^2 \sin 2\theta_2 \sin 2\theta_3}\left[v_1^2 \cos(2\theta_2 - 2\theta_3)\sin 2\theta_2 \sin 2\theta_3 - w^2 \sin^2(2\theta_2 - 2\theta_3)\right] + \frac{2v_1^2}{v^2 w^2}\left[\lambda_{11} w^4 + \lambda_{22} v_2^4 + \lambda_{33} v_3^4 - \bar{\lambda}_{12} v_2^2 w^2 - \bar{\lambda}_{13} v_3^2 w^2 + \bar{\lambda}_{23} v_2^2 v_3^2\right], \tag{A4d}$$

$$(\mathcal{M}^2_{\text{neut}})_{23} = \frac{2\lambda_1 v_2 v_3}{v v_1 w^2 \sin 2\theta_2 \sin 2\theta_3}\left[-w^2 \sin(2\theta_2 - 2\theta_3)(v_2^2 \sin 2\theta_2 \cos 2\theta_3 + v_3^2 \sin 2\theta_3 \cos 2\theta_2) + v_1^2(v_2^2 - v_3^2)\cos(2\theta_2 - 2\theta_3)\sin 2\theta_2 \sin 2\theta_3\right] + \frac{v_1 v_2 v_3}{vw^2}\left[-2\lambda_{22} v_2^2 + 2\lambda_{33} v_3^2 + (\bar{\lambda}_{12} - \bar{\lambda}_{13})w^2 + \bar{\lambda}_{23}(v_2^2 - v_3^2)\right], \tag{A4e}$$

$$(\mathcal{M}^2_{\text{neut}})_{25} = \frac{2\lambda_1 v v_2 v_3}{v_1}\sin(2\theta_2 - 2\theta_3), \tag{A4f}$$

$$(\mathcal{M}^2_{\text{neut}})_{33} = \frac{-4\lambda_1 v_2^2 v_3^2}{w^2}\cos(2\theta_2 - 2\theta_3) + \frac{2v_2^2 v_3^2}{w^2}\left[\lambda_{22} + \lambda_{33} - \bar{\lambda}_{23}\right], \tag{A4g}$$

$$(\mathcal{M}^2_{\text{neut}})_{34} = \frac{-2\lambda_1 v v_2 v_3}{v_1}\sin(2\theta_2 - 2\theta_3), \tag{A4h}$$

$$(\mathcal{M}^2_{\text{neut}})_{44} = \frac{-2\lambda_1 v^2 v_2^2 v_3^2}{v_1^2 w^2 \sin 2\theta_2 \sin 2\theta_3}\sin^2(2\theta_2 - 2\theta_3), \tag{A4i}$$

$$(\mathcal{M}^2_{\text{neut}})_{45} = \frac{-2\lambda_1 v v_2 v_3}{v_1 w^2 \sin 2\theta_2 \sin 2\theta_3}\sin(2\theta_2 - 2\theta_3)\left[v_2^2 \sin 2\theta_2 \cos 2\theta_3 + v_3^2 \sin 2\theta_3 \cos 2\theta_2\right], \tag{A4j}$$

$$(\mathcal{M}^2_{\text{neut}})_{55} = \frac{-2\lambda_1}{w^2 \sin 2\theta_2 \sin 2\theta_3}\left[2v_2^2 v_3^2 \cos(2\theta_2 - 2\theta_3)\sin 2\theta_2 \sin 2\theta_3 + v_2^4 \sin^2 2\theta_2 + v_3^4 \sin^2 2\theta_3\right], \tag{A4k}$$

with $(\mathcal{M}^2_{\text{neut}})_{14} = (\mathcal{M}^2_{\text{neut}})_{15} = (\mathcal{M}^2_{\text{neut}})_{24} = (\mathcal{M}^2_{\text{neut}})_{35} = 0$. Most of these are singular if θ_2 or θ_3 vanishes faster than the other one.

It is also instructive to study the determinant,

$$D_{5\times 5} = \frac{\lambda_1^2 \sin^2(2\theta_2 - 2\theta_3)}{v^2 v_1^4 (v_2^2 + v_3^2)^5 \sin^5 2\theta_2 \sin^5 2\theta_3} F(\theta_2, \theta_3, \ldots), \tag{A5}$$

with

$$F(\theta_2, \theta_3, \ldots) = 64\lambda_1^3 v_2^6 v_3^{10} w^2 \sin^2 2\theta_2 \sin^8 2\theta_3 \tilde{F}_{2,8} + \lambda_1^2 v_2^4 v_3^8 \sin^3 2\theta_2 \sin^7 2\theta_3 \tilde{F}_{3,7} + \lambda_1 v_2^2 v_3^6 \sin^4 2\theta_2 \sin^6 2\theta_3 \tilde{F}_{4,6} + v_2^4 v_3^4 \sin^5 2\theta_2 \sin^5 2\theta_3 \tilde{F}_{5,5} + \{(\theta_2, v_2, \lambda_{22}, \bar{\lambda}_{12}) \leftrightarrow (\theta_3, v_3, \lambda_{33}, \bar{\lambda}_{13})\}, \tag{A6}$$

with $\tilde{F}_{mn}$ regular, homogeneous expansions in the λ's and powers of the VEVs, as well as sines and cosines of the θ's, accompanying the overall factors $\sin^m 2\theta_2 \sin^n 2\theta_3$. Overall, if both θ's are small, $F(\theta_2, \theta_3, \ldots)$ is of order 10 in the θ's, canceling the singularity of the prefactor of Eq. (A5), but leaving an overall dependence on the θ's given by $\sin^2(2\theta_2 - 2\theta_3)$.

The determinant of $\mathcal{M}^2_{\text{neut}}$ has an overall factor of λ_1^2 reflecting the fact that in the absence of the terms in V_{ph} there would be two massless states, originating from the breaking of the $U(1) \times U(1)$ symmetry.

For $\sin(2\theta_2 - 2\theta_3) = 0$ the elements $(\mathcal{M}^2_{\text{neut}})_{25} = (\mathcal{M}^2_{\text{neut}})_{34} = (\mathcal{M}^2_{\text{neut}})_{44} = (\mathcal{M}^2_{\text{neut}})_{45} = 0$, and the mass-squared matrix becomes block diagonal. A 3×3 block will account for mixing among η_1^{HB}, η_2^{HB}, and η_3^{HB}, whereas a 2×2 block will describe a massless χ_2^{HB} and a massive χ_3^{HB}. This model would preserve CP, as already mentioned in Sec. II B. However, there is also another way to achieve factorization, as discussed in Appendix B.

a. Masses of the $U(1) \times U(1)$ pseudo-Goldstone bosons

A nonzero λ_1 explicitly breaks the $U(1) \times U(1)$ symmetry of the potential and turns the two Goldstone bosons into pseudo-Goldstone bosons. The masses of these pseudo-Goldstone bosons can be computed to first order in λ_1 by writing the mass matrix in the symmetry basis as

$$\mathcal{M}^2_{6\times6} = \mathcal{M}^2_{6\times6}\Big|_{\lambda_1=0} + \lambda_1 \frac{\partial \mathcal{M}^2_{6\times6}}{\partial \lambda_1} \tag{A7}$$

$$\equiv \mathcal{M}^2_{(0)} + \lambda_1 \mathcal{M}^2_{(1)} \tag{A8}$$

and applying time-independent perturbation theory. The unperturbed system has a threefold degeneracy corresponding to the $U(1)_Y$ and $U(1) \times U(1)$ Goldstone bosons. Hence, when λ_1 is turned on, the $\mathcal{O}(\lambda_1)$ corrections to the masses of these states are given by the eigenvalues of the perturbation matrix in the degenerate subspace spanned by the three massless states [46],

$$(\mathcal{M}^2_{(1)})_{ij} = \mathbf{n}_i \frac{\partial \mathcal{M}^2}{\partial \lambda_1} \mathbf{n}_j^T, \tag{A9}$$

where $\mathbf{n}_i$ $(i = 1, 2, 3)$ are three linearly independent massless eigenstates of $\mathcal{M}^2_{(0)}$. This matrix has a zero eigenvalue due to the fact that the $U(1)_Y$ Goldstone boson remains massless after λ_1 is turned on. The two remaining eigenvalues yield the masses of the $U(1) \times U(1)$ pseudo-Goldstone bosons at order $\mathcal{O}(\lambda_1)$,

$$m_i^2 = \frac{-\lambda_1}{v_1^2 \sin 2\theta_2 \sin 2\theta_3} \big(v_1^2 v_2^2 \sin^2(2\theta_2) + v_3^2 v_2^2 \sin^2(2\theta_2 - 2\theta_3) + v_1^2 v_3^2 \sin^2(2\theta_3) \pm \Delta \big), \tag{A10a}$$

where

$$\Delta^2 = \big[v_1^2 (v_2^2 \sin^2(2\theta_2) + v_3^2 \sin^2(2\theta_3)) + v_2^2 v_3^2 \sin^2(2\theta_2 - 2\theta_3) \big]^2 - 4 v_1^2 v_2^2 v_3^2 v^2 \sin^2(2\theta_2) \sin^2(2\theta_3) \times \sin^2(2\theta_2 - 2\theta_3). \tag{A10b}$$

Since all masses squared are linear in the λ's, these above expressions are independent of the λ's defining V_0.

It is instructive to compare these values with the simple model discussed in Appendix B for $\theta_3 = -\theta_2$ and $v_3 = v_2$. In that limit, the above results simplify to

$$m_a^2 = 4\lambda_1 v_2^2 \sin^2 2\theta_2, \qquad m_b^2 = \frac{4\lambda_1 v_2^2}{v_1^2} v^2 \cos^2 2\theta_2. \tag{A11}$$

For a discussion, see Appendix B.

APPENDIX B: A MINIMAL (SIMPLE) MODEL

Inspired by Eq. (2.7) we see that a minimal version of the model can be constructed by imposing a symmetry under the interchange

$$\phi_2 \leftrightarrow \phi_3. \tag{B1}$$

This immediately implies

$$m_{22} = m_{33}, \qquad \lambda_2 = \lambda_3, \tag{B2}$$

as well as

$$\lambda_{22} = \lambda_{33}, \qquad \lambda_{12} = \lambda_{13}, \qquad \lambda'_{12} = \lambda'_{13}. \tag{B3}$$

It follows from the minimization conditions (2.4) and (2.6) that, while the moduli of the VEVs are the same, we must have opposite phases,

$$v_2 = v_3, \qquad \theta_2 = -\theta_3. \tag{B4}$$

Obviously, this simple model conserves CP [47] with CP defined as

$$\begin{pmatrix}\langle\phi_1\rangle\\ \langle\phi_2\rangle\\ \langle\phi_3\rangle\end{pmatrix}\xrightarrow{CP}\begin{pmatrix}1&0&0\\0&0&1\\0&1&0\end{pmatrix}\begin{pmatrix}\langle\phi_1^*\rangle\\ \langle\phi_2^*\rangle\\ \langle\phi_3^*\rangle\end{pmatrix}. \tag{B5}$$

Within this framework, the constraints (2.6) can be expressed as

$$\lambda_2 = -2\lambda_1\frac{v_2^2}{v_1^2}\cos(2\theta_2). \tag{B6}$$

1. Charged sector

The mass-squared matrix of the charged sector is found to be given by

$$(\mathcal{M}^2_{\rm ch})_{11} = 2\lambda_1\frac{v_2^2}{v_1^2}v^2\cos^2 2\theta_2 - \frac{1}{2}\lambda'_{12}v^2, \tag{B7a}$$

$$(\mathcal{M}^2_{\rm ch})_{12} = (\mathcal{M}^2_{\rm ch})^*_{21} = -i\lambda_1 v_2^2\frac{v}{v_1}\sin(4\theta_2), \tag{B7b}$$

$$(\mathcal{M}^2_{\rm ch})_{22} = 2\lambda_1 v_2^2\sin^2 2\theta_2 - \frac{1}{2}\lambda'_{12}v_1^2 - \lambda'_{23}v_2^2. \tag{B7c}$$

The two masses are determined by a quadratic equation,

$$m_\pm^2 = \frac{1}{2}\left[a \pm \sqrt{b}\right], \tag{B8}$$

with

$$a = 2\lambda_1\frac{v_2^2}{v_1^2}\left[v^2 - 2\sin^2(2\theta_2)v_2^2\right] - \lambda'_{12}(v_1^2+v_2^2) - \lambda'_{23}v_2^2, \tag{B9}$$

$$b = \frac{v_2^4}{v_1^4}\left\{4\lambda_1^2(v^2 - 2\sin^2 2\theta_2 v_2^2)^2 + 4v_1^2(\lambda'_{12}-\lambda'_{23}) \times\left[2\sin^2 2\theta_2(v_1^2+v_2^2) - v^2\right] + (\lambda'_{12}-\lambda'_{23})^2 v_1^4\right\}. \tag{B10}$$

If we consider the limit $\lambda_1 \to 0$, we find

$$m_\pm^2 \to \frac{1}{2}\left[-\lambda'_{12}(v_1^2+v_2^2\mp v_2^2) - \lambda'_{23}(v_2^2 \pm v_2^2)\right]. \tag{B11}$$

On the other hand, if we make the further assumption that $\lambda'_{12} = \lambda'_{23}$, we find

$$m_\alpha^2 = -\frac{1}{2}\lambda'_{12}v^2, \tag{B12a}$$

$$m_\beta^2 = m_\alpha^2 + \Delta m^2, \tag{B12b}$$

$$\Delta m^2 = \frac{2\lambda_1 v_2^2}{v_1^2}(v_1^2 + 2v_2^2\cos^2 2\theta_3). \tag{B12c}$$

If $\lambda_1 > 0$, we have $m_\beta > m_\alpha$, otherwise the order is inverted. We must require $\lambda'_{12} < 0$.

2. Neutral sector

In the Higgs basis and invoking Eq. (B6), the 5×5 mass-squared matrix takes the form

$$(\mathcal{M}^2_{\rm neut})_{11} = \frac{2}{v^2}\left[-2\lambda_1 v_2^4(1+2\cos^2 2\theta_2) + \lambda_{11}v_1^4 + 2\lambda_{22}v_2^4 + 2\bar\lambda_{12}v_1^2v_2^2 + \bar\lambda_{23}v_2^4\right], \tag{B13a}$$

$$(\mathcal{M}^2_{\rm neut})_{12} = \frac{2\sqrt{2}\lambda_1 v_2^3}{v_1 v^2}(-v_1^2 + 4v_2^2\cos^2 2\theta_2) + \frac{\sqrt{2}v_1v_2}{v^2}\left[-2\lambda_{11}v_1^2 + 2\lambda_{22}v_2^2 + \bar\lambda_{12}(v_1^2 - 2v_2^2) + \bar\lambda_{23}v_2^2\right], \tag{B13b}$$

$$(\mathcal{M}^2_{\rm neut})_{22} = \frac{v_2^2}{v^2}\left[2\lambda_1[-v_1^2 + 2(v_1^2+4v_2^2)\cos^2 2\theta_2] + (4\lambda_{11} + 2\lambda_{22} - 4\bar\lambda_{12} + \bar\lambda_{23})v_1^2\right], \tag{B13c}$$

$$(\mathcal{M}^2_{\rm neut})_{25} = 2\lambda_1 v\frac{v_2^2}{v_1}\sin 4\theta_2, \tag{B13d}$$

$$(\mathcal{M}^2_{\rm neut})_{33} = 2\lambda_1 v_2^2(1-2\cos^2 2\theta_2) + (2\lambda_{22} - \bar\lambda_{23})v_2^2, \tag{B13e}$$

$$(\mathcal{M}^2_{\rm neut})_{34} = -2\lambda_1 v\frac{v_2^2}{v_1}\sin 4\theta_2, \tag{B13f}$$

$$(\mathcal{M}^2_{\rm neut})_{44} = 4\lambda_1 v^2\frac{v_2^2}{v_1^2}\cos^2 2\theta_2, \tag{B13g}$$

$$(\mathcal{M}^2_{\rm neut})_{55} = 4\lambda_1 v_2^2\sin^2 2\theta_2, \tag{B13h}$$

the remaining elements being zero.

3. Factorization

Since the mass-squared matrix for the neutral sector, Eq. (B13), becomes block diagonal, its determinant factorizes. One factor comes from the $\{\eta_1^{\rm HB}, \eta_2^{\rm HB}, \chi_3^{\rm HB}\}$ sector,

$$(\mathcal{M}^2)_{\rm neut,3\times 3} = \begin{pmatrix}(\mathcal{M}^2_{\rm neut})_{11} & (\mathcal{M}^2_{\rm neut})_{12} & (\mathcal{M}^2_{\rm neut})_{15}\\ (\mathcal{M}^2_{\rm neut})_{21} & (\mathcal{M}^2_{\rm neut})_{22} & (\mathcal{M}^2_{\rm neut})_{25}\\ (\mathcal{M}^2_{\rm neut})_{51} & (\mathcal{M}^2_{\rm neut})_{52} & (\mathcal{M}^2_{\rm neut})_{55}\end{pmatrix}, \tag{B14}$$

and the other comes from the $\{\eta_3^{\rm HB}, \chi_2^{\rm HB}\}$ sector,

$$(\mathcal{M}^2)_{\rm neut,2\times 2} = \begin{pmatrix} (\mathcal{M}^2_{\rm neut})_{33} & (\mathcal{M}^2_{\rm neut})_{34} \\ (\mathcal{M}^2_{\rm neut})_{43} & (\mathcal{M}^2_{\rm neut})_{44} \end{pmatrix}. \tag{B15}$$

The two determinants are given by

$$\begin{aligned} D_{3\times 3} = \frac{8\lambda_1 v_2^4 \sin^2(2\theta_2)}{v_1^2} \big[& 8\lambda_1^2 v_2^4 \cos^2 2\theta_2 \\ & - 2\lambda_1 \big[\lambda_{11} v_1^4 + (4\lambda_{22} + 2\bar{\lambda}_{23}) v_2^4 \cos^2 2\theta_2\big] \\ & + v_1^4 (2\lambda_{11}\lambda_{22} + \lambda_{11}\bar{\lambda}_{23} - \bar{\lambda}_{12}^2)\big], \end{aligned} \tag{B16}$$

and

$$D_{2\times 2} = \frac{4\lambda_1 v^2 v_2^4}{v_1^2}(-2\lambda_1 + 2\lambda_{22} - \bar{\lambda}_{23})\cos^2(2\theta_2). \tag{B17}$$

Both of these vanish in the limit of $\lambda_i \to 0$, i.e., when $V_{\rm ph} \to 0$. Furthermore, both determinants are proportional to v_2^4, so if the VEVs of ϕ_2 and ϕ_3 were to vanish, two masses in each sector would vanish. This feature is reflected in the scans of the full model shown in Figs. 3 and 6. There are no points at the origin in the $v_2 \exp(i\theta_2)$ or $v_3 \exp(i\theta_3)$ planes.

4. *CP* conservation

Inspection of the gauge couplings discussed in Sec. III, in particular the Zh_ih_j couplings given by Eq. (3.5), shows that $P_{12} = P_{15} = P_{25} = 0$ and that $P_{34} = 0$, so states within each set have the same *CP*. Furthermore, the nonvanishing ZZh_1, ZZh_2, and ZZh_5 couplings and the vanishing of the ZZh_3 and ZZh_4 couplings confirm the following identification:

$$\eta_1^{\rm HB}, \eta_2^{\rm HB}, \chi_3^{\rm HB} (\text{not}\, \eta_3^{\rm HB}) \quad \text{mix to form } h_1, h_2, h_5, \quad CP \text{ even}, \tag{B18}$$

$$\chi_2^{\rm HB}, \eta_3^{\rm HB} (\text{not}\, \chi_3^{\rm HB}) \quad \text{mix to form } h_3, h_4, \quad CP \text{ odd}, \tag{B19}$$

and, as stated above, *CP* is conserved in this model.[11]

5. The two pseudo-Goldstone bosons

In Appendix 2 A a we discussed the masses of the pseudo-Goldstone bosons to first order in λ_1. For the present simplified model, with $v_3 = v_2$ and $\theta_3 = -\theta_2$, the results for those masses linear in λ_1 simplify to

$$\begin{aligned} m_i^2 = \frac{\lambda_1}{v_1^2 \sin^2 2\theta_2} \big[& 2 v_1^2 v_2^2 \sin^2 2\theta_2 \\ & + 4 v_2^4 \sin^2 2\theta_2 \cos^2 2\theta_2 \pm \Delta\big], \end{aligned} \tag{B20a}$$

$$\Delta^2 = 4 v_2^2 \sin^2 2\theta_2 \big[v_1^2 - 2(v^2 - v_2^2)\cos^2 2\theta_2\big]^2. \tag{B20b}$$

We find the two values

$$m_a^2 = 4\lambda_1 v_2^2 \sin^2 2\theta_2, \qquad m_b^2 = \frac{4\lambda_1 v_2^2}{v_1^2} v^2 \cos^2 2\theta_2. \tag{B21}$$

These mass values are seen to be contained as factors in the above determinants $D_{3\times 3}$ and $D_{2\times 2}$, with m_a^2 being a factor of $D_{3\times 3}$ and m_b^2 a factor of $D_{2\times 2}$. Referring back to the *CP* properties of the 3×3 and the 2×2 blocks, we conclude that in the limit $\lambda_1 \to 0$, then h_a (mass m_a) would be even under *CP* and h_b (mass m_b) would be odd. They become degenerate for

$$|\tan 2\theta_2| = \frac{v}{v_1}, \tag{B22}$$

which is necessarily larger than unity. It follows from the discussion in the previous subsection that such degenerate states would have different *CP*, as they must.

Finally, in the limit $\lambda_1 \to 0$ we find compact expressions for the non-pseudo-Goldstone masses: From the 2×2 block,

$$m_c^2 = (2\lambda_{11} - \bar{\lambda}_{23}) v_2^2, \tag{B23}$$

and from the 3×3 block,

$$m_{d,e}^2 = \frac{\alpha \pm \beta}{2}, \tag{B24}$$

where

$$\alpha = v_2^2(2\lambda_{22} + \bar{\lambda}_{23}) + 2\lambda_{11} v_1^2, \tag{B25}$$

$$\beta = \sqrt{4 v_2^2 v_1^2 (2\bar{\lambda}_{12}^2 - \lambda_{11}(2\lambda_{22} + \bar{\lambda}_{23})) + v_2^4 (2\lambda_{22} + \bar{\lambda}_{23})^2 + 4\lambda_{11}^2 v_1^4}. \tag{B26}$$

[11] However, because of the mixing between η and χ scalar fields, this model becomes *CP* violating when coupled to fermions.

[1] T. D. Lee, A theory of spontaneous T violation, Phys. Rev. D **8**, 1226 (1973).
[2] S. L. Glashow and S. Weinberg, Natural conservation laws for neutral currents, Phys. Rev. D **15**, 1958 (1977).
[3] E. A. Paschos, Diagonal neutral currents, Phys. Rev. D **15**, 1966 (1977).
[4] G. C. Branco and M. N. Rebelo, The Higgs mass in a model with two scalar doublets and spontaneous *CP* violation, Phys. Lett. **160B**, 117 (1985).
[5] S. Weinberg, Gauge theory of *CP* violation, Phys. Rev. Lett. **37**, 657 (1976).
[6] G. C. Branco, Spontaneous *CP* nonconservation and natural flavor conservation: A minimal model, Phys. Rev. D **22**, 2901 (1980).
[7] ACME Collaboration, Improved limit on the electric dipole moment of the electron, Nature (London) **562**, 355 (2018).
[8] G. C. Branco, Spontaneous *CP* violation in theories with more than four quarks, Phys. Rev. Lett. **44**, 504 (1980).
[9] F. J. Botella, G. C. Branco, M. Nebot, and M. N. Rebelo, New physics and evidence for a complex CKM, Nucl. Phys. **B725**, 155 (2005).
[10] J. Charles, A. Hocker, H. Lacker, S. Laplace, F. R. Le Diberder, J. Malcles *et al.* (CKMfitter Group), *CP* violation and the CKM matrix: Assessing the impact of the asymmetric *B* factories, Eur. Phys. J. C **41**, 1 (2005).
[11] J. A. Aguilar-Saavedra, R. Benbrik, S. Heinemeyer, and M. Pérez-Victoria, Handbook of vectorlike quarks: Mixing and single production, Phys. Rev. D **88**, 094010 (2013).
[12] J. M. Alves, G. C. Branco, A. L. Cherchiglia, C. C. Nishi, J. T. Penedo, P. M. F. Pereira *et al.*, Vector-like singlet quarks: A roadmap, arXiv:2304.10561.
[13] I. P. Ivanov and C. C. Nishi, Symmetry breaking patterns in 3HDM, J. High Energy Phys. 01 (2015) 021.
[14] N. Darvishi and A. Pilaftsis, Classifying accidental symmetries in multi-Higgs doublet models, Phys. Rev. D **101**, 095008 (2020).
[15] G. Harris and C. Martin, The roots of a polynomial vary continuously as a function of the coefficients, Proc. Am. Math. Soc. **100**, 390 (1987).
[16] A. M. Sirunyan *et al.* (CMS Collaboration), Constraints on anomalous *HVV* couplings from the production of Higgs bosons decaying to τ lepton pairs, Phys. Rev. D **100**, 112002 (2019).
[17] G. Aad *et al.* (ATLAS Collaboration), Test of *CP* invariance in vector-boson fusion production of the Higgs boson in the $H \to \tau\tau$ channel in proton-proton collisions at s=13 TeV with the ATLAS detector, Phys. Lett. B **805**, 135426 (2020).
[18] A. Pilaftsis, Symmetries for standard model alignment in multi-Higgs doublet models, Phys. Rev. D **93**, 075012 (2016).
[19] P. S. Bhupal Dev and A. Pilaftsis, Maximally symmetric two Higgs doublet model with natural standard model alignment, J. High Energy Phys. 12 (2014) 024.
[20] F. J. Botella and J. P. Silva, Jarlskog-like invariants for theories with scalars and fermions, Phys. Rev. D **51**, 3870 (1995).
[21] G. C. Branco, M. N. Rebelo, and J. I. Silva-Marcos, *CP*-odd invariants in models with several Higgs doublets, Phys. Lett. B **614**, 187 (2005).
[22] J. F. Gunion and H. E. Haber, Conditions for *CP*-violation in the general two-Higgs-doublet model, Phys. Rev. D **72**, 095002 (2005).
[23] R. L. Workman *et al.* (Particle Data Group), Review of particle physics, Prog. Theor. Exp. Phys. **2022**, 083C01 (2022).
[24] B. Grzadkowski, O. M. Ogreid, and P. Osland, Measuring *CP* violation in two-Higgs-doublet models in light of the LHC Higgs data, J. High Energy Phys. 11 (2014) 084.
[25] M. P. Bento, H. E. Haber, J. C. Romão, and J. P. Silva, Multi-Higgs doublet models: Physical parametrization, sum rules and unitarity bounds, J. High Energy Phys. 11 (2017) 095.
[26] A. Tumasyan *et al.* (CMS Collaboration), Analysis of the *CP* structure of the Yukawa coupling between the Higgs boson and τ leptons in proton-proton collisions at $\sqrt{s} = 13$ TeV, J. High Energy Phys. 06 (2022) 012.
[27] D. Fontes, J. C. Romão, R. Santos, and J. P. Silva, Large pseudoscalar Yukawa couplings in the complex 2HDM, J. High Energy Phys. 06 (2015) 060.
[28] B. Grzadkowski, O. M. Ogreid, and P. Osland, Natural multi-Higgs model with dark matter and *CP* violation, Phys. Rev. D **80**, 055013 (2009).
[29] F. S. Faro and I. P. Ivanov, Boundedness from below in the $U(1) \times U(1)$ three-Higgs-doublet model, Phys. Rev. D **100**, 035038 (2019).
[30] M. P. Bento, J. C. Romão, and J. P. Silva, Unitarity bounds for all symmetry-constrained 3HDMs, J. High Energy Phys. 08 (2022) 273.
[31] ATLAS Collaboration, Combined measurements of Higgs boson production and decay using up to 139 fb^{-1} of proton-proton collision data at $\sqrt{s} = 13$ TeV collected with the ATLAS experiment, ATLAS Report No. ATLAS-CONF-2021-053, 2021.
[32] J. Goldstone, Field theories with superconductor solutions, Nuovo Cimento **19**, 154 (1961).
[33] J. Goldstone, A. Salam, and S. Weinberg, Broken symmetries, Phys. Rev. **127**, 965 (1962).
[34] R. Plantey, O. M. Ogreid, P. Osland, M. N. Rebelo, and M. A. Solberg, Light scalars in the Weinberg 3HDM potential with spontaneous *CP* violation, Proc. Sci. DISCRETE2020-2021 (**2022**) 064 [arXiv:2209.06499].
[35] LEP Higgs Working Group for Higgs Boson Searches, OPAL, ALEPH, DELPHI, L3 Collaborations, Search for the standard model Higgs boson at LEP, Phys. Lett. B **565**, 61 (2003).
[36] P. A. McNamara and S. L. Wu, The Higgs particle in the standard model: Experimental results from LEP, Rep. Prog. Phys. **65**, 465 (2002).
[37] I. de Medeiros Varzielas and I. P. Ivanov, Recognizing symmetries in a 3HDM in a basis-independent way, Phys. Rev. D **100**, 015008 (2019).
[38] N. Darvishi, M. R. Masouminia, and A. Pilaftsis, Maximally symmetric three-Higgs-doublet model, Phys. Rev. D **104**, 115017 (2021).
[39] A. M. Sirunyan *et al.* (CMS Collaboration), Search for a standard model-like Higgs boson in the mass range between 70 and 110 GeV in the diphoton final state in proton-proton collisions at $\sqrt{s} = 8$ and 13 TeV, Phys. Lett. B **793**, 320 (2019).
[40] S. Heinemeyer, C. Li, F. Lika, G. Moortgat-Pick, and S. Paasch, A 96 GeV Higgs Boson in the 2HDMS: e^+e^- collider prospects, in *International Workshop on Future*

Linear Colliders, arXiv:2105.11189 (DESY Report No. DESY-21-077, 2021).
[41] T. Biekötter, S. Heinemeyer, and G. Weiglein, Mounting evidence for a 95 GeV Higgs boson, J. High Energy Phys. 08 (2022) 201.
[42] T. Biekötter, S. Heinemeyer, and G. Weiglein, Excesses in the low-mass Higgs-boson search and the W-boson mass measurement, Eur. Phys. J. C **83**, 450 (2023).
[43] R. Barbieri, L. J. Hall, and V. S. Rychkov, Improved naturalness with a heavy Higgs: An alternative road to LHC physics, Phys. Rev. D **74**, 015007 (2006).
[44] N. G. Deshpande and E. Ma, Pattern of symmetry breaking with two Higgs doublets, Phys. Rev. D **18**, 2574 (1978).
[45] Q.-H. Cao, E. Ma, and G. Rajasekaran, Observing the dark scalar doublet and its impact on the standard-model Higgs boson at colliders, Phys. Rev. D **76**, 095011 (2007).
[46] J. J. Sakurai and J. Napolitano, *Modern Quantum Mechanics*, Quantum Physics, Quantum Information and Quantum Computation (Cambridge University Press, Cambridge, England, 2020).
[47] G. C. Branco, J. M. Gerard, and W. Grimus, Geometrical T violation, Phys. Lett. **136B**, 383 (1984).